Journal of
Marine Science and Engineering

MDPI

Article

New Insights about Upwelling Trends off the Portuguese Coast: An ERA5 Dataset Analysis

Spallou Ferreira [1], Magda Sousa [2], Ana Picado [2], Nuno Vaz [2] and João Miguel Dias [2,*]

1 Physics Department, Campus de Santiago, University of Aveiro, 3810-193 Aveiro, Portugal
2 CESAM, Centre for Environmental and Marine Studies, Physics Department, Campus de Santiago, University of Aveiro, 3810-193 Aveiro, Portugal
* Correspondence: joao.dias@ua.pt

Abstract: In recent decades, several studies have highlighted the importance of the temporal and spatial structure of upwelling in defining the high levels of productivity of coastal upwelling systems. This work intends to assess the temporal and spatial trends of upwelling along the west and south Portuguese coasts from 1979 to 2020, comparing the patterns between these regions. Two different methodologies to calculate the upwelling indexes (UI), based on wind and sea surface temperature (SST) data, were applied to relate the wind-induced upwelling-favourable conditions (UI_{ET}) with the expected response on superficial waters, as indicated by the SST patterns (UI_{SST}). The upwelling-favourable conditions are quite consistent and more frequent and intense on the west coast than on the south coast. Spatially, it was verified from the UI_{ET} that upwelling-favourable conditions are more intense in association with the main west coast capes and that there is an intensification of favourable winds towards Cape São Vicente, both on the west and south coasts. Seasonally, upwelling-favourable UI_{ET} was found to be more consistent in the summer on both coasts. However, it also exists in the winter months. In terms of interannual variations, it should be highlighted that between 1992 and 2005 more intense favourable conditions and an apparent change in the seasonality after 2015 were found. Although some of the results derived from the UI_{ET} are corroborated by the UI_{SST} (namely, the main spatial trends and interannual variations in the upwelling intensity), several uncertainties are associated with the last index that interfere with its interpretation. For future works, it is advisable to develop a more robust SST-based index that can circumvent the uncertainties pointed out in the present study.

Keywords: Ekman transport; Iberian Peninsula; SST; upwelling

Citation: Ferreira, S.; Sousa, M.; Picado, A.; Vaz, N.; Dias, J.M. New Insights about Upwelling Trends off the Portuguese Coast: An ERA5 Dataset Analysis. *J. Mar. Sci. Eng.* **2022**, *10*, 1849. https://doi.org/10.3390/jmse10121849

Academic Editor: Alvise Benetazzo

Received: 27 October 2022
Accepted: 26 November 2022
Published: 1 December 2022

1. Introduction

The northwest coast of the Iberian Peninsula (IP) has been extensively studied during recent decades and has important hydrologic and biogeochemical activity, mainly attributable to coastal upwelling processes [1–4]. Works carried out around the Galician coast [5–7] have shown that the upwelling frequency and intensity are influenced by the coastal orientation, which modulates the wind direction and intensity, changing the prevalence of upwelling-favourable conditions in each coastal region. Along the western coast, these upwelling events are more probable than along the northern coast due to different coastal orientations [6–8]. Although this coastal upwelling is a spring–summer process, it can also be observed in autumn–winter [9–20]. These studies have shown that the mean long-term patterns of summer and winter wind fields may not be representative of particular years, as upwelling patterns can also be persistent in winter. Additionally, wind patterns may alternate, briefly producing episodes of upwelling at the northern or western coast, or a combined pattern may occur producing weak upwelling on both coasts [5].

Although there are fewer studies focused on the southern coast of the IP, the transitions observed from the northern coast to the western coast of the IP are also applicable in terms of wind patterns, when comparing the western coast with the southern coast. Due to the different orientations of the western and southern coasts (Figure 1), northerly winds produce upwelling off the western coast, whereas westerly winds induce this phenomenon off the southern coast. Strong northerly winds are associated with the northward displacement of the Azores high-pressure cell and the weakening of the Iceland low-pressure cell [21], resulting in a well-defined upwelling season between March and September [22]. It should be noted that the Azores high-pressure cell is associated with a large-scale clockwise circulation, where the west Portuguese coast is affected by the east side of this circulation, which is characterized by northerly winds. The westerly winds off the southern Portuguese coast occur in summer due to the establishment of a low-pressure centre of thermal origin over the IP. As the orientation of the coast changes abruptly at Cape Sao Vicente, both northerly and westerly winds are upwelling-favourable in this region [21].

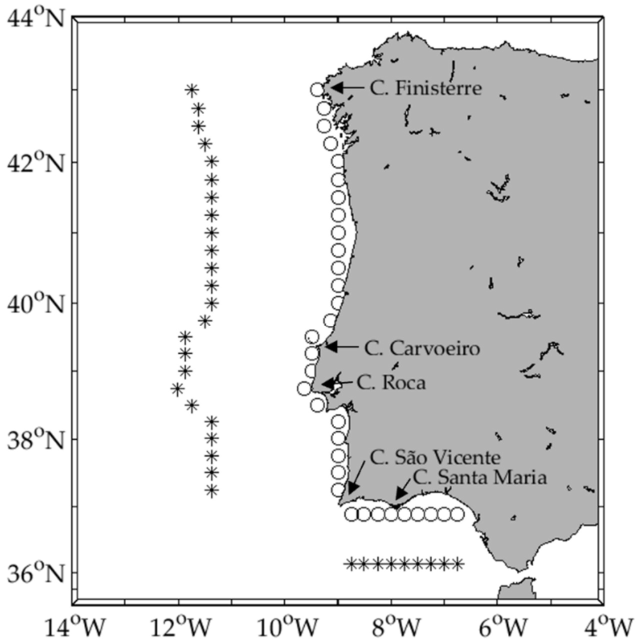

Figure 1. Map of the study area. The circles represent the nearshore points where both wind and SST data were obtained. The asterisks represent the offshore points where SST data were obtained.

As stated by [23], studies evaluating upwelling trends based on sea surface temperature (SST) data have been somewhat arbitrary in the choice of upwelling indexes, as they depend on the purpose of the study they serve and on the data used. Most of the studies that compared wind-induced circulation with the effects on SST [12,15,18,22] estimated upwelling occurrences only based on the difference of SST between oceanic and coastal waters and found, on the western coast of the IP, higher occurrences in late summer, with maximum occurrences in September instead of August (differently than what is indicated by wind-driven circulation). A more recent study focused only on SST data, though with a more elaborated upwelling index, and found higher upwelling occurrences between July and September, centred in August [23]. Therefore, a better understanding of long-term coastal upwelling variability is essential to adequately assess the consequences of this process. For such understanding, the calculation of upwelling indexes is very useful and can be used alongside other environmental data. Moreover, it is very important to assess the differences and similarities of this phenomenon along adjacent and perpendicular coastlines. The present study investigates the spatial and temporal patterns of upwelling along the western coast of the IP and the southern Portuguese coast, using the more traditional upwelling indexes based on wind-induced circulation as well as the upwelling effect on SST, based on long-term reanalysis data. Section 3 presents the main features and trends that were found, and the discussion analyses their relevance and reliability along with covering the new insights achieved. Possible causes for the less reliable results are also discussed and are presented in Section 5, along with suggestions for future work that are worthy of investigation to improve the methods adopted here and the results that were found.

2. Materials and Methods

For this work, data were extracted from the "ERA5 monthly averaged data on single levels from 1979 to present" dataset [24], the 10 m u-component (u) and 10 m v-component (v) of wind and the SST for 42 years, from January 1979 to December 2020. The data were extracted from 36° N to 45° N and from 4° W to 14° W in a regular grid with a spatial resolution of 0.125° × 0.125°. According to [25], which analysed the performance of several reanalysis products in very heterogeneous locations worldwide, ERA5 is the best dataset for assessing wind intensity on offshore and flat onshore locations. Thus, ERA5 allows the evaluation of seasonal and long-term trends in coastal upwelling.

Two different methodologies to calculate upwelling indexes (UI) based on wind and SST data were applied. To quantify the influence of wind stress in generating superficial currents, Ekman transport was calculated. The longitudinal (Q_x) and meridional (Q_y) components of the Ekman transport were obtained through the longitudinal and meridional wind components and considering water density, ρ_w = 1025 kg m^{-3}, and air density, ρ_a = 1.2 kg m^{-3}, as follows:

$$Q_x = \frac{\rho_a C_d}{\rho_w f}\left(u^2 + v^2\right)^{1/2} v \quad (1)$$

$$Q_y = -\frac{\rho_a C_d}{\rho_w f}\left(u^2 + v^2\right)^{1/2} u \quad (2)$$

where f is the Coriolis parameter, defined as a function of the vertical component of Earth's angular velocity, Ω, and of latitude, θ, as follows f = 2Ωsin(θ). C_d is the drag coefficient, computed using wind speed at 10 m (U_{10}), as parameterized by [26]:

$$C_d = \frac{2.7}{U_{10}} + 0.142 + 0.076U_{10} \quad (3)$$

The UI that allows the quantification of wind-induced circulation favourable to coastal upwelling (UI_{ET}) is the component of Ekman transport perpendicular to the coast, with positive values offshore [27]. Thus, UI_{ET} can be calculated with the longitudinal and meridional components of the Ekman transport through the expression $UI_{ET} = -sin(\theta)Q_x + cos(\theta)Q_y$ where $\theta = \varphi - \pi/2$, and φ is the angle defined by an unitary vector perpendicular to the coastline and pointing seaward [6]. Although the angles of the Portuguese west and south coasts are not exactly constant along both sides, macroscopically the west coast can be considered perpendicular [8] and the south coast parallel to the equator. Thus, UI_{ET} was calculated for 24 points located approximately 0.125° (~14 km) offshore the west coast and for 9 points located approximately 0.125° offshore the south coast (Figure 1, circles). Positive (negative) UI_{ET} values indicate favourable (unfavourable) upwelling conditions.

To quantify the coastal upwelling from the SST values, the difference between nearshore (Figure 1, circles) and offshore (Figure 1, asterisks) SST (UI_{SST}) was calculated. The distance between points is 80 km for the south coast and 200 km for the west coast, to avoid the influence of upwelling filaments that usually extends to long distances offshore the west coast (Figure 1). Since the water temperature at the surface varies with latitude due to solar differential heating, to obtain the south coast UI_{SST} this meridional temperature gradient (ΔT/Δy) should be subtracted from the difference obtained between near-shore and offshore points. To estimate the ΔT/Δy, 3 points at latitudes 36.0, 36.5 and 37.0° N were considered along 6 different longitudes between 11° W and 13.5° W (where SST should be less affected by upwelling occurrences), spaced 0.5° apart, and the SST difference between each point and the adjacent point located at higher latitude was calculated. Although the ΔT/Δy obtained is not constant longitudinally (it increases towards the west), a mean value of −0.44 °C per 1° of latitude was considered. Since offshore points are 0.75° S from the nearshore points, the value to be subtracted from the difference between the nearshore and offshore points (or added to the offshore points) is −0.33 °C. This method, used to estimate the UI_{SST} on the south coast, was inspired by the procedure adopted by [15] to estimate the UI_{SST} on the north coast of the IP. In this way, negative (positive) UI_{SST} values indicate the occurrence (non-occurrence) of coastal upwelling.

To analyse spatial variability, the percentages of upwelling-favourable UI_{ET} were calculated for each coastal point, considering the number of months where the UI_{ET} was higher than 100 $m^3\ s^{-1}\ km^{-1}$, with relation to the total number of months of the period under study. Percentages of UI_{SST} indicating upwelling occurrences were also calculated for each coastal point, considering the months where the UI_{SST} was lower than −0.6 °C.

Taking into account the annual variability, for each coast, spatially averaged values of UI_{ET} and UI_{SST} were firstly obtained (on the south coast, only the points from Cape Santa Maria to the west were considered). Then, using the same criteria as for the spatial variability, the percentages of upwelling-favourable UI_{ET} and the percentages of UI_{SST} indicating upwelling occurrences were calculated for each month, with relation to the total number of years of the period under study.

3. Results

3.1. Upwelling Patterns

The results presented in this section summarize quite well the main spatial and temporal patterns of UI_{ET} and UI_{SST} obtained from the application of the methodology previously described. To analyse the spatial variability, Figure 2 shows the percentage of upwelling-favourable conditions based on the Ekman transport and SST indexes. A higher tendency of both favourable conditions and occurrences of upwelling from north to south, on the west coast, and from east to west, on the south coast, is noticeable, as the percentages of UI_{ET} (Figure 2a) and UI_{SST} (Figure 2b) increase in these directions. Despite this general trend, there are also local maximums where the percentages of the indexes are higher. Percentages of favourable UI_{ET} are higher at latitudes associated with the main capes, namely Finisterre cape (43° N), between Carvoeiro and Roca capes (38.5 to 39.5° N), and São Vincente cape (37° N). The percentages of UI_{SST} are also higher between Carvoeiro and Roca capes and towards São Vincente cape but not at Finisterre cape. Instead, they are higher between 41° N and 42° N.

Regarding the annual variation of the UI_{ET} percentages (Figure 2), it is noticeable that, on the west coast, the summer months present upwelling-favourable conditions more frequently, with a maximum in August (81%). There are two other peaks of high percentages in March (60%) and December (48%). The month with the lowest frequency of upwelling-favourable conditions is January (24%), followed by November (28%). On the south coast, similar to the west coast, there are two peaks of high percentages in August (57%) and December (52%). However, the rest of the annual pattern is quite different, since the winter months (all above 40%, with a maximum of 52%, in February) present upwelling-favourable conditions more frequently than the summer months. There is a decrease in upwelling-favourable conditions towards the months of transition from spring to summer and from summer to autumn, namely May–June (21%) and September (26%). Analysing the annual variability of UI_{SST} (Figure 2d), it is possible to observe a similar seasonal cycle on both coasts. The higher percentages occur in August, September and October (100% on the west coast versus ~90% on the south coast) and decrease towards the minimum of April (14% on the west coast versus 24% on the south coast). The main difference between the coasts lies in the higher frequencies of occurrences on the west coast and in the asymmetry of values around the months of higher percentages. In other words, the increase in percentages towards the months of higher percentages is sharper on the west coast than on the south coast, and after these months the decrease is sharper on the south coast than on the west coast. On the south coast, in addition to the annual cycle, there is a peak in winter (February, 38%).

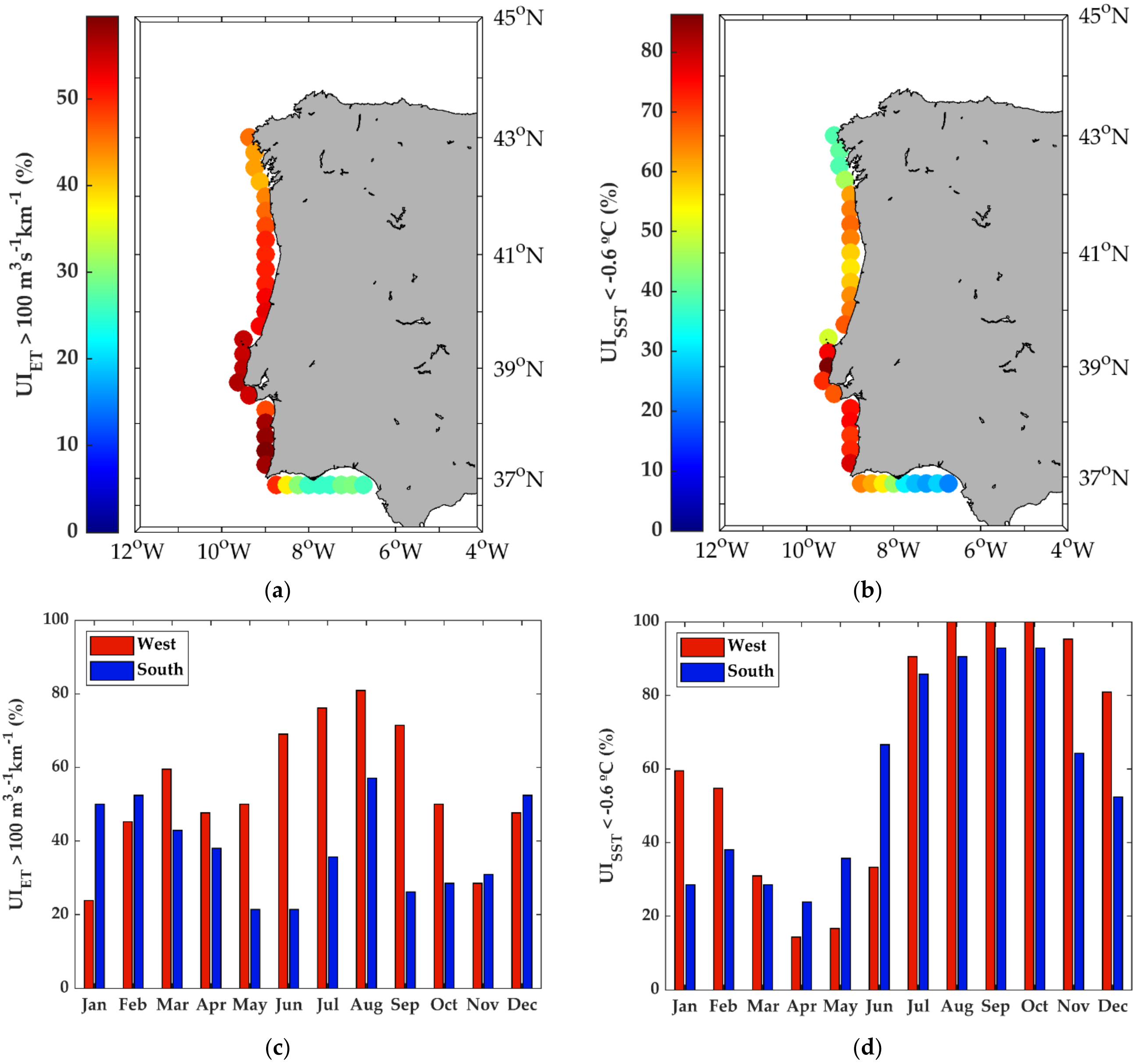

Figure 2. Percentage of upwelling-favourable conditions (occurrences) based on Ekman transport and SST indexes: (**a**) percentages of months with UI_{ET} values higher than 100 m^3 s^{-1} km^{-1}, for each point; (**b**) percentages of months with UI_{SST} values lower than −0.6 °C, for each coastal point; (**c**) percentages of spatially averaged UI_{ET} values higher than 100 m^3 s^{-1} km^{-1}, for each month of the year, on the west and south coasts; (**d**) percentages of spatially averaged UI_{SST} values lower than −0.6 °C, for each month of the year, on the west and south coasts.

3.2. Evolution of the Upwelling Index Based on Ekman Transport

The temporal evolution of UI_{ET} from 1979 to 2020 along the western and southern coasts is depicted in Figure 3. From this interannual evolution, a different behaviour between UI_{ET} for the western and southern coasts was observed, with more short-term variability along the western coast than along the southern one, without a clear annual cycle or pattern. To better understand this evolution, and as the spatial variability along each coast is low, time series were obtained by spatially averaging the temporal evolution of UI_{ET} from 1979 to 2020 on each coast (Figure 4). Although upwelling-favourable conditions on the west coast are more consistent, frequent positive indexes were also found on the south coast, inclusively, with sporadic values (3600 m^3 s^{-1} km^{-1}, in April 1996, and

5500 m^3 s^{-1} km^{-1}, in March 2018) higher than the absolute maximum observed on the west coast (3400 m^3 s^{-1} km^{-1} in February 2019, at 42.5° N).

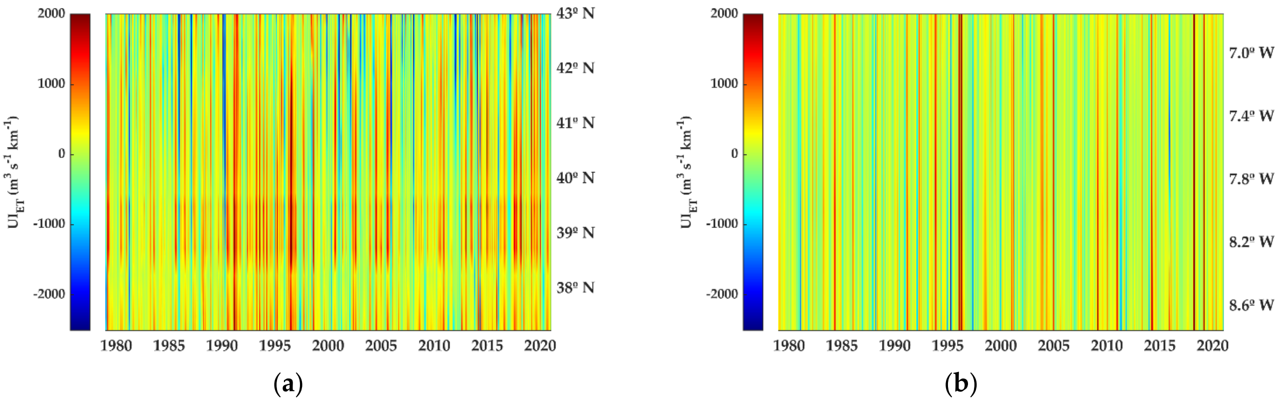

Figure 3. Evolution of UI$_{ET}$ (m^3 s^{-1} km^{-1}) over the period 1979–2020 along the Portuguese (**a**) west coast and (**b**) south coast.

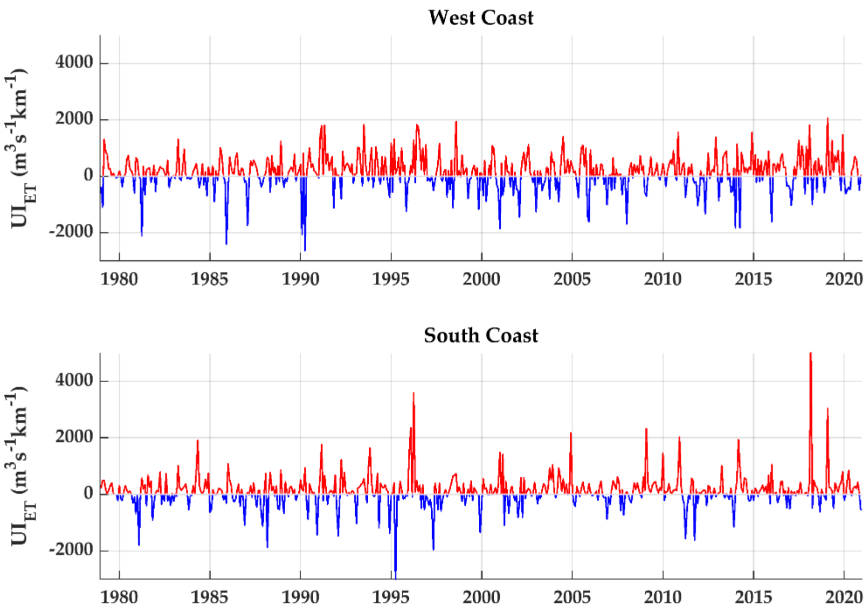

Figure 4. Spatial averages of the evolution of UI$_{ET}$ (m^3 s^{-1} km^{-1}) on the Portuguese west and south coasts over the period 1979–2020. The red line represents positive values, and the blue line represents negative values.

Figure 5 presents the spatial averages of each month from 1979 to 2020, for both coasts. A 3-year moving average was considered to be better for observing the overall behaviour. On the west coast (Figure 5a), the months from June to September present high values of UI$_{ET}$ in a very regular way over the years. In some years, February, March, April, May and December also present upwelling-favourable conditions, but this rarely happens simultaneously in the same year. February only starts to present high UI$_{ET}$ consistently from 2014 onwards. As shown in the previous section, November is the month that less frequently presents upwelling-favourable conditions. However, lower values of UI$_{ET}$ are observed in January, February and April. On the southern coast, the most regular months are July and August, with positive intensities mostly. February, March, April and December are the months contributing the highest "anomalous" UI$_{ET}$ values.

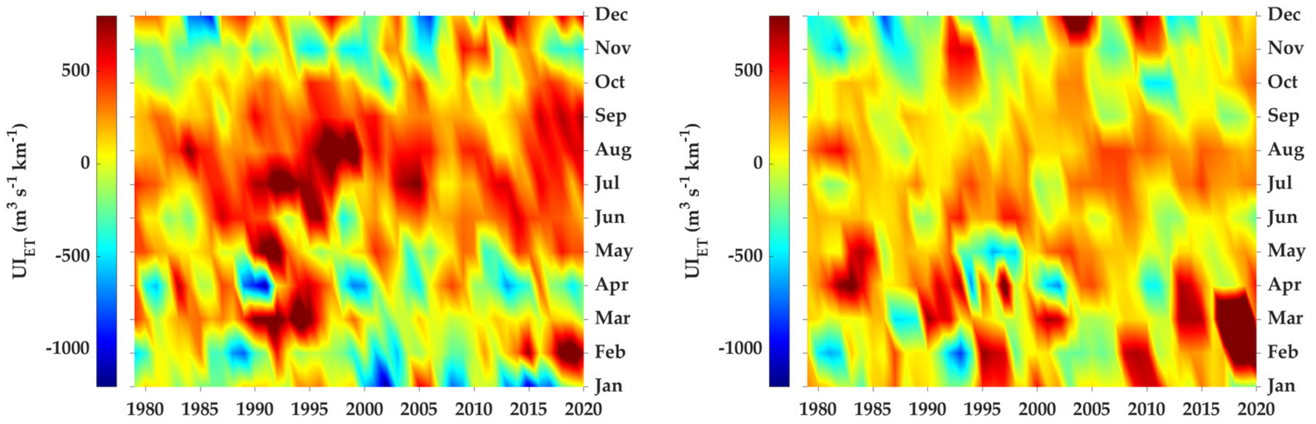

(**a**) (**b**)

Figure 5. Monthly evolution of UI_{ET} (m^3 s^{-1} km^{-1}), from 1979 to 2020, obtained by representing the spatial average of each month in function of the years: (**a**) west coast and (**b**) south coast.

3.3. Evolution of the Upwelling Index Based on SST

The temporal evolution of UI_{SST} from 1979 to 2020 along the western and southern coasts is shown in Figure 6. The annual cycle of UI_{SST} is well-defined and similar between the west and south coasts, but the conditions indicating upwelling occurrence (negative UI_{SST}) are higher on the west coast (lower values below −2 °C) than on the south coast (lower values above −2 °C). Unlike the UI_{ET} evolution shown in Figure 3b, there is a high spatial variation of UI_{SST} along the south coast (Figure 6b). The range of values presents lower limits to the west (−2–0 °C), while these limits are higher to the east (−1–1 °C). To evaluate their temporal evolution, a spatial average of the UI_{SST} for both west (all points are considered) and south (only points from Cape Santa Maria to the west are considered) coasts was performed (Figure 7). On the south coast, the spatial variation is not low enough that an average can be considered representative of the whole coast. Figure 7 makes the annual cycle of UI_{SST} even clearer, and negative values are almost always present (meaning that, at the surface, coastal waters tend to be always colder than oceanic waters). UI_{SST} is mostly negative, varying between −3 °C and 0 °C, being positive values very rare. On the west coast, the highest UI_{SST} occurred in May 1997 (0.6 °C) and the lowest in September 2020 (−4 °C). On the south coast, the maximum UI_{SST} was registered in July 2013 (0.5 °C), and the minimum was in September 2020 (−4.6 °C). In the last decade, the annual cycle of UI_{SST} showed changes on both coasts, presenting lower values on the west coast and losing definition on the south coast.

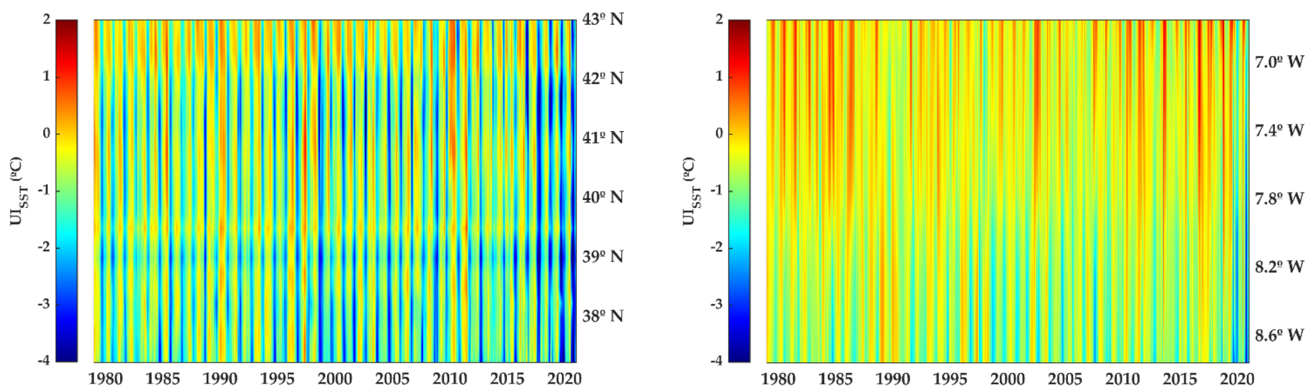

(**a**) (**b**)

Figure 6. Evolution of UI_{SST} (°C) over the period 1979–2020 on the Portuguese (**a**) west coast and (**b**) south coast.

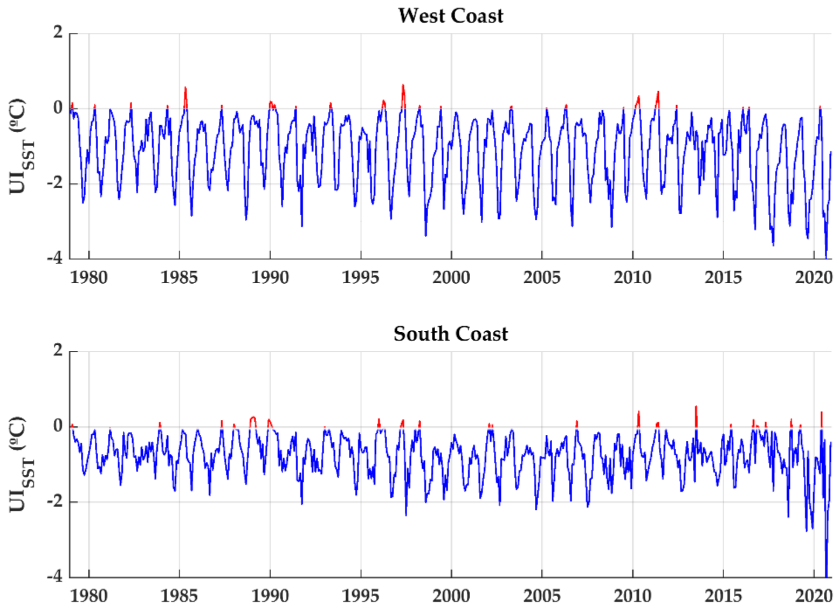

Figure 7. Spatial averages of the evolution of UI_{SST} (°C) on the Portuguese west and south coasts over the period 1979–2020. The red line represents positive values, and the blue line represents negative values.

To better evaluate the monthly trends of UI_{SST} over the years, their spatial averages are represented in diagrams (Figure 8). On the west coast, negative UI_{SST} values occur from July to December, with the lowest values being observed from August to October and with September presenting the lowest UI_{SST} values of all months. Higher UI_{SST} values (near zero) occur mostly from March to June and also in January and February. On the south coast, the annual pattern is similar, although less intense, with the lower values observed from July to November not being as low as the lowest values observed on the west coast. The months with higher values differ slightly from the ones found for the west coast, with June presenting the lowest values and December the highest ones. Thus, the period with a higher UI_{SST} on the south coast is from December to May instead of January to June (as on the west coast). From 1979 to 2015, small interannual variations of these patterns are observed, and the period from 1993 to 2005 showed the lowest UI_{SST} values (higher upwelling occurrence) on both coasts. On the other hand, from 2015 to 2020, the annual cycle suffered an alteration. On the west coast, the months with a lower UI_{SST} extend from August–September–October (typical pattern) to July–August–September–October–November, and the months of December, January, February and March also present lower-than-normal UI_{SST} values. On the south coast, the annual cycle also changed from 2015 onwards, though in a different way. In fact, lower-than-normal UI_{SST} values are observed in February and March of 2015–2018 and in July to December of 2020, while UI_{SST} values higher-than-normal are observed in July of 2015–2017 and in September of 2018. The general lowering of UI_{SST} from 2015 to 2020 is also observable in Figures 6 and 7.

Figure 9 shows the climatological normal of the nearshore and offshore spatial averages of the SST, which will later be useful for the discussion of the observed annual cycle of the UI_{SST}. For the offshore points, on both coasts, the highest values of SST are observed from August to October (~20 °C/22 °C at the west/south coasts), with a maximum in September (20.5 °C/22.1 °C), while the lowest SST values are observed from February to April, with a minimum in March (14.3 °C/16.2 °C). The same pattern is detected in the colder nearshore waters, though with a lower magnitude (~6 °C offshore versus ~4 °C nearshore). On the west coast, the difference between the nearshore and offshore SST is at its maximum in September (2.4 °C), which decreases towards May, when the difference is much lower (0.4 °C). On the south coast, the difference between the nearshore and offshore SST is also higher in September (1.8 °C or 1.5 °C, considering $\Delta T/\Delta y$) but is more constant during the cold months (0.7 °C or 0.3 °C), unlike on the west coast. One important aspect to highlight is the higher difference between the nearshore and offshore SST due to the higher offshore values in September.

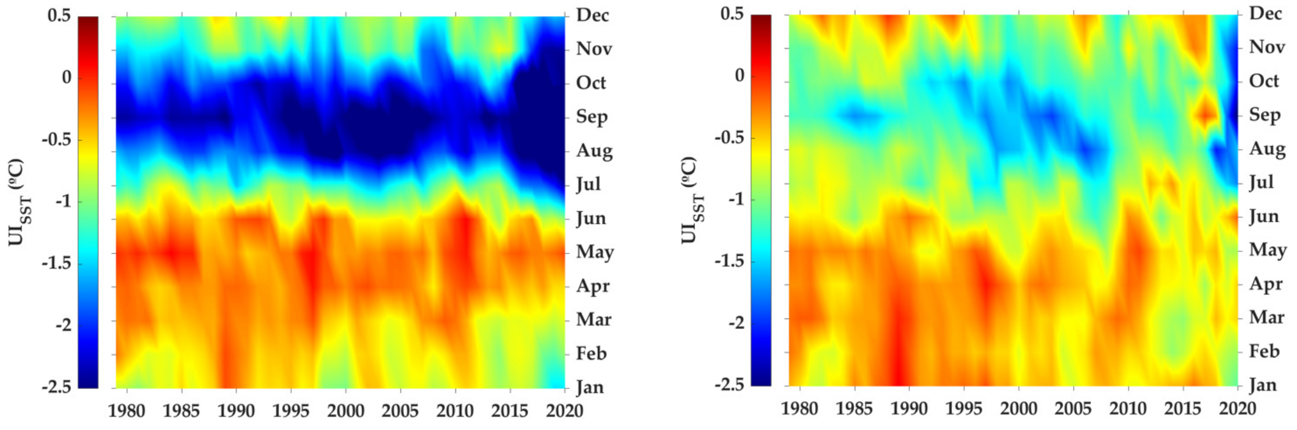

Figure 8. Monthly evolutions of UI_{SST} (°C) from 1979 to 2020: (**a**) west coast and (**b**) south coast.

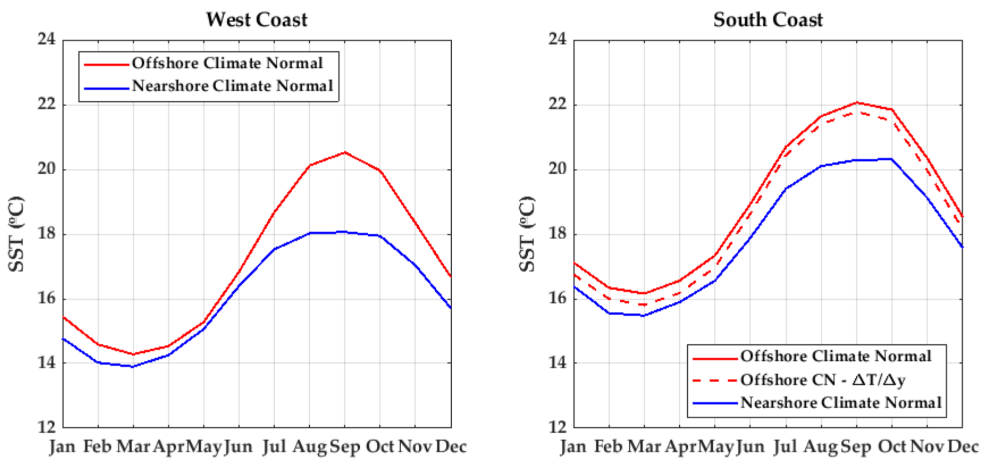

Figure 9. Climatological normals of nearshore and offshore spatial averages of the Portuguese west and south coasts, considering the entire period covered by the data.

After analysing Figure 9, it was hypothesized that SST climatology might influence the information given by UI_{SST}. Given the need to evaluate that influence, a new estimation of the spatially averaged UI_{SST} temporal evolution is presented in Figure 10. It was obtained by subtracting the nearshore and offshore climate normal from the corresponding nearshore and offshore series, before calculating the difference between the series. Here, the positive and negative values of UI_{SST} will not indicate downwelling or upwelling occurrence, instead they will indicate the months where the difference between nearshore and offshore SST deviated from the climatological normal. The cross-correlation between the centred UI_{SST} series (from now on also referred to as c-UI_{SST}) and the spatially averaged temporal series of UI_{ET} was computed. A linear fit of the nearshore and offshore temporal series was also included for the interpretation of the interannual variability of UI_{SST}. The results show that, on the west coast, there is no trend in nearshore SST, while the offshore SST shows a clear positive slope, indicating an increase in offshore SST over the years (Figure 10). On the south coast, both the nearshore and offshore linear fits have a positive slope that indicates an increasing trend of SST over the years, with the highest increase occurring offshore.

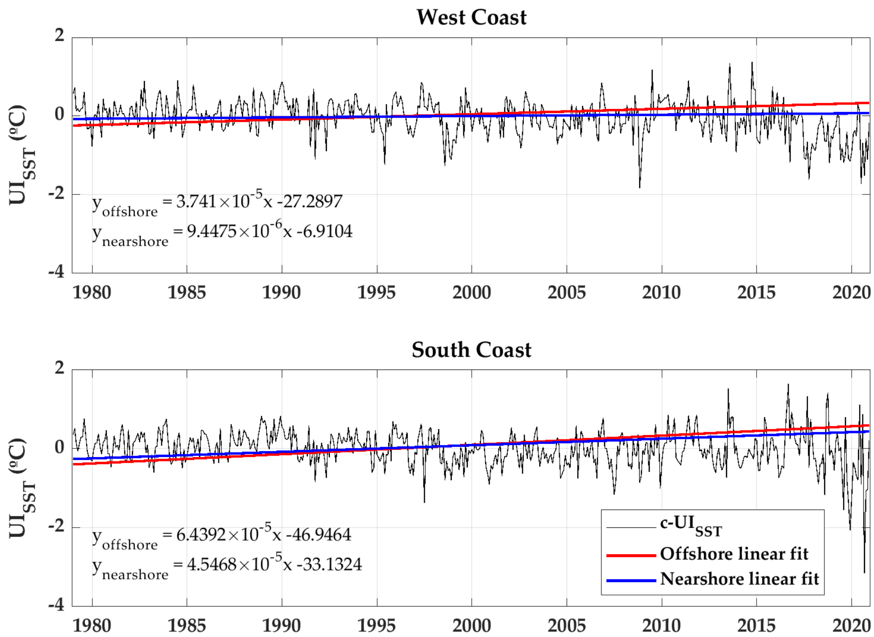

Figure 10. Annual evolution of UI_{SST} (°C) on the Portuguese west coast and south coasts over the period 1979–2020, considering climatological normals of the nearshore and offshore spatially averaged temporal series. The blue and red lines represent simple linear fits of the nearshore and offshore spatial averages, respectively.

To determine the correlation and lag between the UI_{ET} and UI_{SST} and between the UI_{ET} and c-UI_{SST} time series, the cross-correlation for delay periods of 12 months was calculated, for both the west and south coasts (Figure 11). Between the UI_{ET} and UI_{SST} time series, the value of the correlation coefficient corresponding to the maximum modulus is −0.25 at a 1-month lag for the west coast and −0.15 at a 5-month lag for the south coast. On the other hand, while correlating the UI_{ET} to the c-UI_{SST} time series, the correlation coefficient of the maximum modulus is obtained at 0 lag on both coasts, with values of −0.17 for the west coast and −0.13 for the south coast. It is also noticeable that the spike of negative correlation at a 5-month lag on the south coast is still observed.

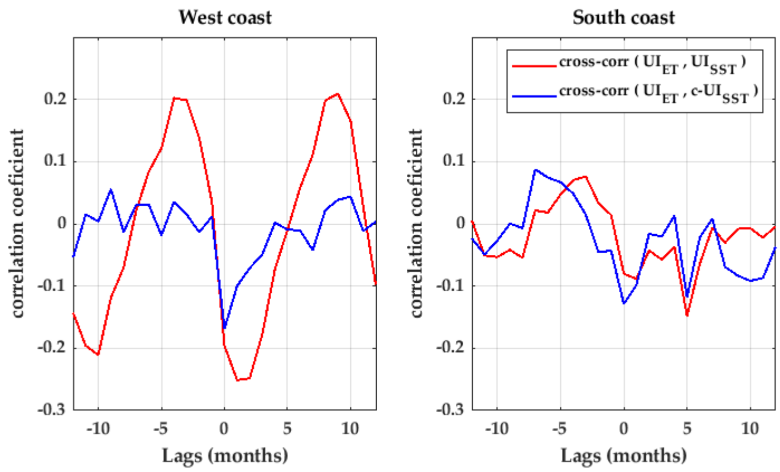

Figure 11. Cross-correlation between the UI_{ET} and the UI_{SST} time series (red line) and between the UI_{ET} and the c-UI_{SST} time series (blue line).

4. Discussion

To understand the main spatial and temporal trends of upwelling along the west and south Portuguese coasts, the wind and SST data from ERA5 were used to compute the UI for a 42-year period (January 1979 to December 2020). Two different methodologies were applied, one based on wind data (UI_{ET}) and the other one based on SST (UI_{SST}), to relate the wind-induced upwelling-favourable conditions with the expected response on superficial waters, as indicated by the SST patterns.

In terms of spatial variability, the results show a higher intensity of UI_{ET} from north to south on the west coast and towards Cape São Vicente on the south coast (Figure 2a). Moreover, upwelling-favourable UI_{ET} is higher at the latitudes associated with the main capes. This pattern is consistent with the Ekman pumping results described by Alvarez et al. [8]. Generally, regarding $UI_{SST,}$ there is a north–south direction decrease along the west coast (Figure 2b). However, this may not be an indicator of a higher upwelling intensity towards the south, rather representing an offshore differential of solar heating. In fact, according to a study carried out by Miranda et al. [28], if the differential of solar heating is disregarded, SST patterns indicate higher upwelling occurrences on the northwest coast of the IP.

On the west coast, the general increase in UI_{ET} and UI_{SST}, indicating an upwelling occurrence towards the south, may not be completely related because, as explained before, the UI_{SST} may suffer from the too-simplistic approach used here for its calculation. However, it would make sense that a higher UI_{ET} towards the south leads to a higher response by the UI_{SST} in the same direction. In addition to that, the concordance of both indices about a higher upwelling intensity near the main capes is more reliable and in agreement with the existing knowledge [8]. A difference between indexes that must be noted is that UI_{SST} depicts the region of a higher upwelling occurrence between 41° N and 42° N that is not observable from the UI_{ET}. The higher percentage of occurrence found for UI_{SST} might be erroneous, as a plume of fresh water is dominant at these latitudes [29], which in the winter presents a lower SST than the oceanic waters.

The UI_{ET} seasonality obtained on the west coast is quite similar to the one presented in [15], although there is a difference in January and December, which present unfavourable conditions for upwelling in [15], while in the present study these months showed mostly favourable conditions. The high unpredictability of the upwelling conditions in the winter months found in the present work agrees with the results obtained by [8]. These authors found considerable differences in these months while performing decadal means of the annual cycles of UI_{ET}. It is also observable from Figure 5 that the extreme negative and positive UI_{ET} values are more likely to occur in the winter months.

From Figure 8, it is observed that from July to December the west coast presents the lowest UI_{SST}, with values below −1 °C and a minimum in September, which is almost always below −2.5 °C (identical to those obtained by Alvarez et al. [15]). The main differences between upwelling occurrences for the south coast and the west coast are the lower frequency of upwelling occurrence (Figure 2d), the lower intensity of these events (Figure 7) and the displacement of the season of more consistent upwelling occurrences between June to November (Figures 2d and 8). The main annual patterns of UI_{ET} and UI_{SST} are in agreement with the results obtained by [21], as these authors found that off the west coast, during summer, wind stress is the dominant, dynamic forcing mechanism, resulting in the prevalence of an upwelling regime, while off the south coast the upwelling events are intermittent. Thus, the characteristics of the west coast upwelling suggest a typical pattern of an eastern boundary current upwelling system, but this is somewhat modified on the south coast [21]. The same work also depicted that there is a filament of cold water flowing eastwards of Cape São Vicente, which is independent of upwelling events on the southern coast. This filament constitutes the southward extension of the equatorward coastal jet associated with the west coast upwelling and overshoots the cape. This must be taken into account, as upwelling-favourable winds on the south coast (westerly winds) are also favourable for the transport of the west coast upwelling filament along the south coast.

From the comparison of the seasonal variation of UI_{ET} and UI_{SST}, it is expected that months with higher upwelling-favourable conditions (higher UI_{ET} and lower UI_{SST}) occur almost simultaneously. Previous studies around the northwestern coast of the IP proved that upwelled water can be easily identified when upwelling-favourable conditions persist for more than 3–4 days [15,30,31]. Considering this short response time, no delay is expected between the wind forcing and the observed effects on the superficial water properties, especially when considering monthly averaged data. Although, on both coasts, a time lag is observed between UI_{ET} and UI_{SST}. Figures 5 and 8 indicate highly upwelling-favourable conditions centred within July and August for UI_{ET} and centred in September for UI_{SST}. This lag between UI_{ET} and UI_{SST} was also observed in previous works where UI_{SST} was obtained only from the difference between coastal and oceanic SSTs [12,15,18,22].

To understand the UI_{SST} pattern, climate normals of the offshore and nearshore SSTs have been determined. From this analysis, it has been found that offshore waters present a higher SST in September, while nearshore there is no significant variability between August, September and October. Thus, the differences between nearshore and offshore SSTs will always be greater in September than in August or October, due to the higher values of SST in ocean waters but not due to the greater occurrence of upwelling. Indeed, the climatology of SST has a clear impact on the annual cycle of UI_{SST}, interfering with the identification of the intense upwelling months. A recent study focused on a long-term analysis of upwelling using SST data, with a more elaborated index, and found that upwelling is more intense in August on the western Portuguese coast and in July on the southern Portuguese coast [23].

On the west coast, the interannual evolution of UI_{ET} over the period under study is very similar to that obtained by [8,15] (for the comparable period from 1979 to 2006/2008), as there is a period with higher UI_{ET} intensities between 1992 and 2005. In 2016, it appears that the season of upwelling-favourable conditions expands to a greater number of months (from May to October) and that September becomes the summer month with higher upwelling-favourable conditions. In the winter months, February also starts to show unprecedented high upwelling-favourable conditions. Interannual variations in the south coast are not clear, but higher-than-normal UI_{ET} values are observed in March and February between 2016 and 2020.

The results obtained for the UI_{SST} evolution along the west coast show a pattern very similar to the one obtained by [15] in the northwestern segment of the IP from 1985 to 2008. As for UI_{ET}, an alteration in the annual cycle of UI_{SST} was registered in recent years. After 2016, UI_{SST} started presenting lower values than in the precedent years (Figure 7). In addition to that, on the west coast, the months with a lower UI_{SST} extend from August–September–October (typical pattern) to July–August–September–October–November, and the months of December, January, February and March also present lower-than-normal UI_{SST} values (Figure 8a). On the south coast, the annual cycle has also showed changes in recent years, though differently, as lower-than-normal UI_{SST} values were observed in February and March of 2015–2018 and in July to December of 2020, while a higher-than-normal UI_{SST} was observed in July of 2015–2017 and in September of 2018 (Figure 8b).

The principal factor that must have contributed to a lower UI_{SST} in the last decade is the augment of months with a higher UI_{ET}. At the same time, from the linear fits of the offshore and nearshore time series (Figure 10), it is observed that the offshore waters have suffered a greater increase in SST than the nearshore waters. Thus, the lower UI_{SST} values in recent years may not be necessarily (or fully) linked to more favourable conditions for upwelling occurrences. In addition to this, it should be taken into account that the observational methodologies and instruments used currently are more robust than in the past. Therefore, since ERA5 combines historical observations into global estimates using advanced modelling and data assimilation systems, the UI interannual variability observed from 2015 could be related to the different acquisition methods.

Conclusions about the evolution of upwelling trends over the years should be taken carefully, as it is not yet consensual if coastal upwelling events should intensify or attenuate with global warming. Some studies predict an increase in coastal upwelling intensity with global warming, since higher temperature gradients between land and sea lead to more intense equatorward winds (upwelling-favourable conditions) on the west coasts of the continents [28,32,33]. On the other hand, [23,34] concluded that the upwelling of the western Iberia coast had weakened since 1940.

5. Conclusions

The present work aimed to analyse the main temporal and spatial tendencies of upwelling off the Portuguese coast. Wind and SST data from ERA5 were used to compute the UI along the west and south coasts between January 1979 and December 2020. Two different methodologies to relate the wind-induced upwelling-favourable conditions (UI_{ET}) with the expected response on superficial waters, as indicated by the SST patterns (UI_{SST}), were applied.

On the west coast, the upwelling-favourable conditions are quite consistent and more frequent and intense than on the south coast. Spatially, it was verified from the UI_{ET} that the more-intense upwelling-favourable conditions are associated with the main west coast capes and that there is an intensification of favourable winds towards Cape São Vicente, both on the west and south coasts. Seasonally, upwelling-favourable UI_{ET} was found to be more consistent in summer on both coasts. However, it also occurs in the winter months. In terms of interannual variations, the period in which there were more intense upwelling-favourable conditions, between 1992 and 2005, should be highlighted, as should an apparent change in seasonality after 2015 (mainly for February and September, which present more favourable conditions compared to the typical patterns). Although some of the information that was collected by the UI_{ET} is corroborated by the UI_{SST} (namely the main spatial trends and interannual variations in the intensity of upwelling), several uncertainties are associated with UI_{SST}, interfering with its interpretation.

- The analysis of the UI_{SST} on the Portuguese west coast revealed an increase in occurrences from north to south. However, the lower values of the UI_{SST} in the south may be related to the higher offshore waters' SST and not to the higher occurrence of coastal upwelling.
- Since the UI_{SST} is based only on the SST difference between the coastal and offshore waters, upwelling occurrences can be erroneously accounted for due to the presence of cold-water masses along the coast, with an existence that is not generated by upwelling events.
- There is a one-month lag between the UI_{ET} and the UI_{SST}, which was not expected due to the rapid response of coastal waters to upwelling-favourable winds. An analysis of the climatology of oceanic and coastal waters allowed for the conclusion that the greatest differences in SST, which are recorded in September, are due to the higher temperatures of the offshore waters and not to a greater occurrence of upwelling.

Overall, the main findings showed that coastal upwelling is not the only factor leading to the temperature differences between coastal and offshore waters. Other forcings that lead to temperature differences throughout the year (differential heating of surface waters, generation of freshwater plumes of fluvial origin or other water masses transported by surface currents) or between years (e.g., an increase in SST due to global warming) also determine the differences in SST between coastal waters and oceanic waters. Thus, one of the main conclusions drawn from this work is that UI_{SST} cannot be considered as being just a reflection of the occurrence of coastal upwelling. On the other hand, UI_{ET} is a very useful index to assess the favourable conditions for upwelling.

For future works, it is recommended that in addition to the methodology followed here, data analysis with a higher temporal resolution is worthy of being researched to investigate whether a greater accuracy in the relationship between UI_{SST} and wind conditions can be found. Additionally, it is advisable to develop and use a more robust index in the future that can circumvent the uncertainties highlighted in the present study.

Author Contributions: Conceptualization: M.S. and J.M.D.; methodology: S.F., M.S., A.P. and J.M.D.; software: S.F., M.S. and A.P.; validation: S.F., M.S. and A.P.; formal analysis: S.F., M.S. and A.P.; investigation: S.F., M.S., A.P. and J.M.D.; resources: J.M.D.; writing—original draft preparation: S.F., M.S., A.P., N.V. and J.M.D.; writing—review and editing: S.F., M.S., A.P., N.V. and J.M.D.; supervision: J.M.D. and M.S.; funding acquisition: J.M.D. All authors have read and agreed to the published version of the manuscript.

Funding: Thanks are due to FCT/MCTES for the financial support to CESAM (UIDP/50017/2020+UIDB/50017/2020+ LA/P/0094/2020) through national funds.

Institutional Review Board Statement: Not applicable.

Informed Consent Statement: Not applicable.

Data Availability Statement: Not applicable.

Conflicts of Interest: The authors declare no conflict of interest.

References

1. Botas, J.A.; Fernandez, E.; Bode, A.; Anadon, R. A persistent upwelling off the Central Cantabrian Coast (Bay of Biscay). *Estuar. Coast. Shelf Sci.* **1990**, *30*, 185–199. [CrossRef]
2. Borja, A.; Uriarte, A.; Egaña, J.; Motos, L.; Valencia, V. Relationships between anchovy (Engraulis encrasicolus) recruitment and environment in the Bay of Biscay (1967–1996). *Fish. Oceanogr.* **1998**, *7*, 375–380. [CrossRef]
3. Borja, A.; Fontán, A.; Sáenz, J.; Valencia, V. Climate, oceanography, and recruitment: The case of the Bay of Biscay anchovy (Engraulis encrasicolus). *Fish. Oceanogr.* **2008**, *17*, 477–493. [CrossRef]
4. Bode, A.; Varela, M.; Casas, B.; González, N. Intrusions of eastern North Atlantic central waters and phytoplankton in the north and northwestern Iberian shelf during spring. *J. Mar. Syst.* **2002**, *36*, 197–218. [CrossRef]
5. Torres, R.; Barton, E.D.; Miller, P.; Fanjul, E.A. Spatial patterns of wind and sea surface temperature in the Galician upwelling region. *J. Geophys. Res. Ocean.* **2003**, *108*, 1–14. [CrossRef]
6. Gómez-Gesteira, M.; Moreira, C.; Alvarez, I.; De Castro, M. Ekman transport along the Galician coast (northwest Spain) calculated from forecasted winds. *J. Geophys. Res. Ocean.* **2006**, *111*. [CrossRef]
7. Alvarez, I.; Gómez-Gesteira, M.; DeCastro, M.; Novoa, E.M. Ekman transport along the Galician Coast (NW, Spain) calculated from QuikSCAT winds. *J. Mar. Syst.* **2008**, *72*, 101–115. [CrossRef]
8. Alvarez, I.; Gómez-Gesteira, M.; DeCastro, M.; Dias, J.M. Spatiotemporal evolution of upwelling regime along the western coast of the Iberian Peninsula. *J. Geophys. Res.* **2008**, *113*. [CrossRef]
9. Santos, A.M.P.; Borges, M.D.F.; Groom, S. Sardine and horse mackerel recruitment and upwelling off Portugal. *ICES J. Mar. Sci.* **2001**, *58*, 589–596. [CrossRef]
10. Santos, A.M.P.; Peliz, A.; Dubert, J.; Oliveira, P.B.; Angélico, M.M.; Ré, P. Impact of a winter upwelling event on the distribution and transport of sardine (Sardina pilchardus) eggs and larvae off western Iberia: A retention mechanism. *Cont. Shelf Res.* **2004**, *24*, 149–165. [CrossRef]
11. Varela, M.; Álvarez-Ossorio, M.T.; Bode, A.; Prego, R.; Bernárdez, P.; Garcia-Soto, C. The effects of a winter upwelling on biogeochemical and planktonic components in an area close to the Galician Upwelling Core: The Sound of Corcubión (NW Spain). *J. Sea Res.* **2010**, *64*, 260–272. [CrossRef]
12. Picado, A.; Alvarez, I.; Vaz, N.; Dias, J.M. Chlorophyll concentration along the northwestern coast of the Iberian Peninsula vs. atmosphere-ocean-land conditions. *J. Coast. Res.* **2013**, 2047–2052. [CrossRef]
13. Alvarez, I.; DeCastro, M.; Prego, R.; Gómez-Gesteira, M. Hydrographic characterization of a winter-upwelling event in the Ria of Pontevedra (NW Spain). *Estuar. Coast. Shelf Sci.* **2003**, *56*, 869–876. [CrossRef]
14. Alvarez, I.; Ospina-Alvarez, N.; Pazos, I.; DeCastro, M.; Bernardez, P.; Campos, M.J.; Gomez-Gesteira, J.L.; Alvarez-Ossorio, M.T.; Varela, M.; Gomez-Gesteira, M.; et al. A winter upwelling event in the Northern Galician Rias: Frequency and oceanographic implications. *Estuar. Coast. Shelf Sci.* **2009**, *82*, 573–582. [CrossRef]
15. Alvarez, I.; Gomez-Gesteira, M.; DeCastro, M.; Lorenzo, M.N.; Crespo, A.J.C.; Dias, J.M. Comparative analysis of upwelling influence between the western and northern coast of the Iberian Peninsula. *Cont. Shelf Res.* **2010**, *31*, 388–399. [CrossRef]
16. Borges, M.d.F.; Santos, A.M.P.; Crato, N.; Mendes, H.; Mota, B. Sardine regime shifts off Portugal: A time series analysis of catches and wind conditions. *Sci. Mar.* **2003**, *67*, 235–244.
17. DeCastro, M.; Dale, A.W.; Gómez-Gesteira, M.; Prego, R.; Alvarez, I. Hydrographic and atmospheric analysis of an autumnal upwelling event in the Ria of Vigo (NW Iberian Peninsula). *Estuar. Coast. Shelf Sci.* **2006**, *68*, 529–537. [CrossRef]
18. DeCastro, M.; Gomez-Gesteira, M.; Alvarez, I.; Lorenzo, M.; Cabanas, J.M.; Prego, R.; Crespo, A.J.C. Characterization of fall-winter upwelling recurrence along the Galician western coast (NW Spain) from 2000 to 2005: Dependence on atmospheric forcing. *J. Mar. Syst.* **2008**, *72*, 145–158. [CrossRef]
19. Prego, R.; Guzmán-Zuñiga, D.; Varela, M.; deCastro, M.; Gómez-Gesteira, M. Consequences of winter upwelling events on biogeochemical and phytoplankton patterns in a western Galician ria (NW Iberian peninsula). *Estuar. Coast. Shelf Sci.* **2007**, *73*, 409–422. [CrossRef]
20. Picado, A.; Alvarez, I.; Vaz, N.; Varela, R.; Gomez-Gesteira, M.; Dias, J.M. Assessment of chlorophyll variability along the northwestern coast of Iberian Peninsula. *J. Sea Res.* **2014**, *93*, 2–11. [CrossRef]
21. Relvas, P.; Barton, E.D. Mesoscale patterns in the Cape São Vicente (Iberian Peninsula) upwelling region. *J. Geophys. Res.* **2002**, *107*, 28-1–28-23. [CrossRef]
22. Fiúza, A.F.d.G.; de Macedo, M.E.; Guerreiro, M.R. Climatological space and time variation of the Portuguese coastal upwelling. *Oceanol. Acta* **1982**, *5*, 31–40.

23. Leitão, F.; Baptista, V.; Vieira, V.; Silva, P.L.; Relvas, P.; Teodósio, M.A. A 60-year time series analyses of the upwelling along the Portuguese coast. *Water* **2019**, *11*, 1285. [CrossRef]
24. COPERNICUS. Available online: https://cds.climate.copernicus.eu/ (accessed on 26 January 2021).
25. Gualtieri, G. Analysing the uncertainties of reanalysis data used for wind resource assessment: A critical review. *Renew. Sustain. Energy Rev.* **2022**, *167*, 112741. [CrossRef]
26. Large, W.G.; Yeager, S. Diurnal to Decadal Global Forcing For Ocean and Sea-Ice Models: The Data Sets and Flux Climatologies. *NCAR Tech. Note* **2004**. [CrossRef]
27. Bakun, A. *Coastal Upwelling Indices, West Coast of North America, 1946–1971*; Superintendent of Documents. U.S. Government Printing Office: Washington, DC, USA, 1973.
28. Miranda, P.M.A.; Alves, J.M.R.; Serra, N. Climate change and upwelling: Response of Iberian upwelling to atmospheric forcing in a regional climate scenario. *Clim. Dyn.* **2013**, *40*, 2813–2824. [CrossRef]
29. Mendes, R.; Sousa, M.C.; DeCastro, M.; Gómez-Gesteira, M.; Dias, J.M. New insights into the Western Iberian Buoyant Plume: Interaction between the Douro and Minho River plumes under winter conditions. *Prog. Oceanogr.* **2016**, *141*, 30–43. [CrossRef]
30. Alvarez-Salgado, X.A.; Gago, J.; Míguez, B.M.; Gilcoto, M.; Pérez, F.F. Surface Waters of the NW Iberian Margin: Upwelling on the Shelf versus Outwelling of Upwelled Waters from the Rías Baixas. *Estuar. Coast. Shelf Sci.* **2000**, *51*, 821–837. [CrossRef]
31. Alvarez, I.; de Castro, M.; Gomez-Gesteira, M.; Prego, R. Inter- and intra-annual analysis of the salinity and temperature evolution in the Galician Rías Baixas-ocean boundary (northwest Spain). *J. Geophys. Res. Ocean.* **2005**, *110*, 1–14. [CrossRef]
32. Bakun, A. Global greenhouse effects, multi-decadal wind trends, and potential impacts on coastal pelagic fish populations. *ICES Mar. Sci. Symp.* **1992**, *195*, 316–325.
33. Bakun, A.; Field, D.B.; Redondo-Rodriguez, A.; Weeks, S.J. Greenhouse gas, upwelling-favorable winds, and the future of coastal ocean upwelling ecosystems. *Glob. Chang. Biol.* **2009**, *16*, 1213–1228. [CrossRef]
34. Lemos, R.T.; Pires, H.O. The upwelling regime off the west Portuguese coast, 1941–2000. *Int. J. Climatol.* **2004**, *24*, 511–524. [CrossRef]